Letters

IOP Publishing Semiconductor Science and Technology

Semicond. Sci. Technol. **34** (2019) 10LT01 (5pp) https://doi.org/10.1088/1361-6641/ab40e7

Letter

On the predictive, quantitative properties of the amphoteric native defect model

Stefan P Svensson[1], Wendy L Sarney[1], William A Beck[1], Leonardo Hsu[2] and Wladek Walukiewicz[3,4]

[1] CCDC Army Research Laboratory, 2800 Powder Mill Rd, Adelphi, Maryland 20783, United States of America
[2] Department of Chemistry and Physics, Santa Rosa Junior College, Santa Rosa, CA 95401, United States of America
[3] Materials Sciences Division, Lawrence Berkeley National Laboratory, Berkeley, CA 94720, United States of America
[4] Department of Materials Science and Engineering, University of California at Berkeley, Berkeley CA 94720, United States of America

E-mail: Stefan.P.Svensson.civ@mail.mil

Received 9 July 2019, revised 19 August 2019
Accepted for publication 3 September 2019
Published 17 September 2019

Abstract

The amphoteric native defect model phenomenologically explains and categorizes observed background doping concentrations and accounts for the doping limitations in compound semiconductors. Here, we test and verify the model's capabilities as a quantitative, predictive tool. We demonstrate that the nature, (donor or acceptor), of non-stoichiometry related vacancy-like defects in the (Al,Ga,In)(As,Sb) system is determined by the position of the intrinsic Fermi energy, E_{Fi} at the growth temperature relative to the Fermi level stabilization energy, E_{FS}, a universal energy reference located at 4.9 eV below the vacuum level. We show that a dramatic and predictable conduction type-flip from n- to p-type occurs when E_{Fi} is deliberately shifted from below to above E_{FS}.

Keywords: compound semiconductor, doping, amphoteric defect

(Some figures may appear in colour only in the online journal)

Compound semiconductors represent a class of materials with wide-ranging applications. As information about their basic properties became increasingly available, there has been a continuing desire, spanning many decades, to organize and find commonalities to predict properties of their more complex alloys, as well as the expected behaviors of hetero-junctions made from combinations of them.

The known relationships between bandgaps and lattice constants infer the possible alloys and hetero-structures that may combine without forming misfit dislocations. The functionality of the hetero-junctions is critically dependent on the relative position of the conduction and valence bands in the two constituents, and the same is true for the related surface barriers.

In an early attempt at organizing Schottky barrier height data, McCaldin *et al* [1] reviewed previous work and proposed the 'common-anion-rule', based on the observation that the valence band edges (VBE) of compounds with common anions seemed to line up at the same energies relative a reference Fermi level of Au. They also observed that the valence band energies scaled with the electro-negativity of the anion. Furthermore, this picture showed the relative positions of the band gaps and provided an early summary of the relative line-ups of the gaps. By no means a complete picture, a substantial body of work on band line-up theories [2] followed.

Controlled bipolar doping is one of the critical properties determining potential applications of compound

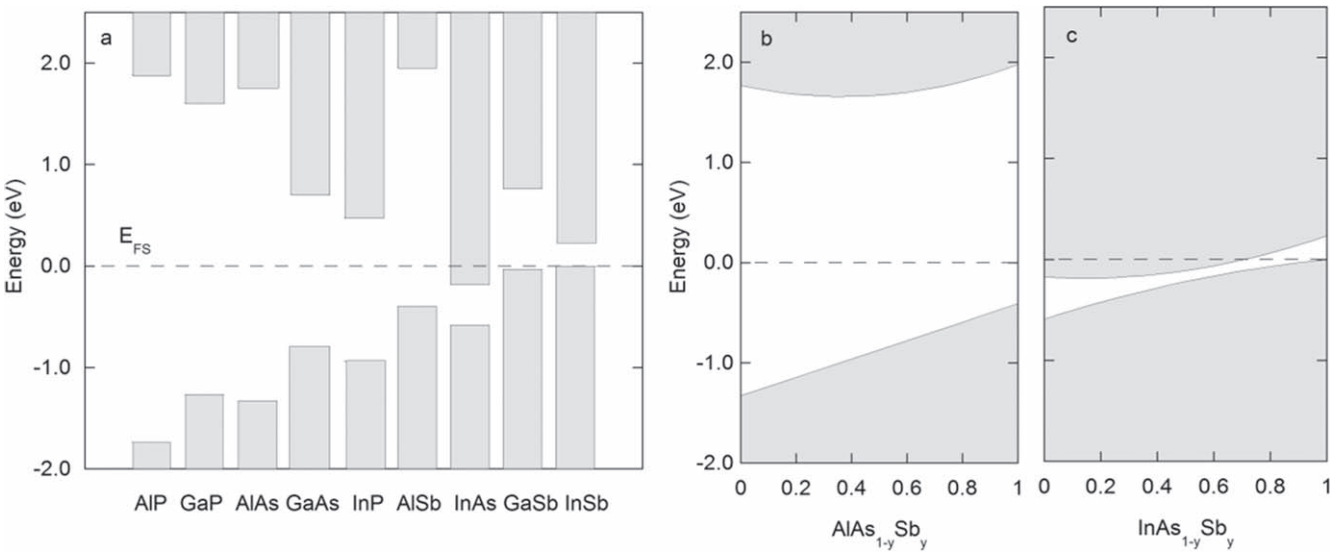

Figure 1. Conduction and valence band edges for binary III–V-compounds (a) and the ternary alloys AlAsSb (b) and InAsSb (c). The energy scale references the InSb valence band edge [10] with E_{FS} assumed to be at zero energy (see text).

semiconductors. Many semiconductors exhibit clear proclivity towards n-type conductivity and in some instances, it is impossible to achieve bipolar conductivity. Although this is especially acute problem for wide gap semiconductors, some narrow gap compounds also exhibit a preference for a specific type of doping. Thus as-grown, undoped GaSb shows a p-type conductivity [3] whereas as-grown, undoped InN with similar band gap is always n-type [4].

In the framework of the relative band line-ups, this doping behavior of semiconductors was explained by Walukiewicz [5–7] with the amphoteric native defect model (ADM). The formation energy and the nature (donor or acceptor) of vacancy-like dangling bond defects are determined by the location of the Fermi energy, E_F relative to a universal energy reference, so called, Fermi-stabilization level, E_{FS}, positioned 4.9 eV below the vacuum level [7] (see figure 1(a)). It should be noted that the E_{FS} energy coincides with the previously introduced charge neutrality level (CNL) and the branch point energy which are the concepts invoked in the pining of the Fermi energy at metal/semiconductor interfaces [8, 9]. The background doping type can then be predicted by the position of E_F relative to E_{FS}. Specifically, the material is expected to exhibit donor (acceptor) defects if the Fermi-level during the material synthesis is above (below) E_{FS}.

Recently the model explained a light-controlled defect formation in III–V compounds [11] and transient optoelectronic properties of hybrid organic inorganic perovskite materials [12]. The ADM has been used to successfully describe the doping behavior of wide gap semiconductors in which there is a large difference between E_F in n-type and p-type doped material [7] and some of these semiconductors exhibit only one type of conductivity. In contrast, narrow band gap semiconductors show bipolar conductivity, as there is only a small energy difference between E_F in n-type and p-type material.

Here we show that the compositional dependence of the residual conductivity of undoped narrow gap (Ga/Al)InAsSb alloys can be explained by an engineered evolution of the intrinsic Fermi energy relative to E_{FS}.

(Ga/Al)InAsSb provides a near ideal semiconductor system to test the ADM. Figures 1(b), (c) show band positions and E_{FS} for AlAsSb and InAsSb. We can observe that E_{FS} is above the conduction band edge (CBE) in the narrow-bandgap alloy for Sb compositions ranging from zero to close to 70%. In the wide-bandgap AlAsSb alloy E_{FS} is in the lower half of the gap for all compositions. Hence, by adding Al (or Ga) to InAsSb it is possible to tune the E_{FS} position continuously from the conduction band down into the bandgap. We would then expect that the shift should have significant effect on the nature of dominant defects and thus also on the type of conductivity.

We have previously verified both the predicted n-type background doping, as well as the surface electron accumulation in InAsSb [13]. By examining temperature-dependent Hall effect data we [14] determined that a resonant donor level was situated 8.7 meV *above* the CBE in InAsSb with a mole fraction of $x = 0.43$. Because of the location of the donor level, the free electron concentration at low temperatures was lower than the donor density.

To verify the ADM predictions, we used synchronized dynamic molecular beam epitaxy (MBE) to produce bulk alloy layers on virtual substrates [15], ensuring threading dislocation densities below $10^6\,cm^{-2}$. The structures were analyzed with high-resolution x-ray diffraction. The lattice constants of the samples are plotted in figure 2, showing the level of control of the process. Further details of the materials synthesis of the quaternary alloys and their bandgaps will be presented elsewhere [16].

Hall effect samples were prepared, and data collected and analyzed as described in [14]. The temperature dependent carrier concentration results are shown in figure 3 for the case of aluminum alloying. The gallium case looks qualitatively

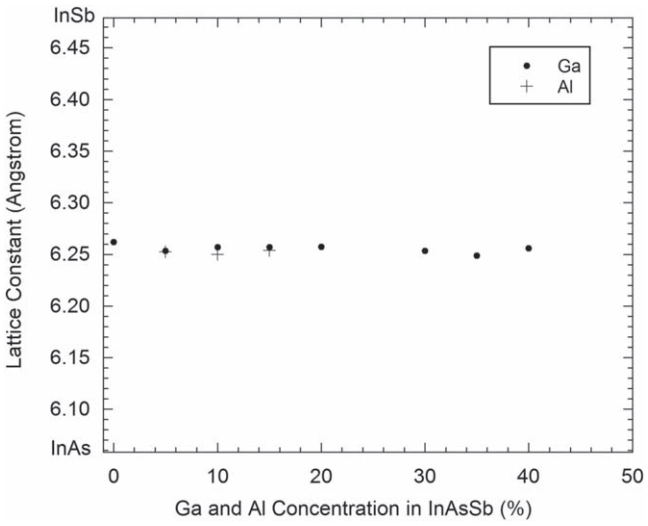

Figure 2. Lattice constants of the GaAlInAs and AlInAsSb samples used in the investigation.

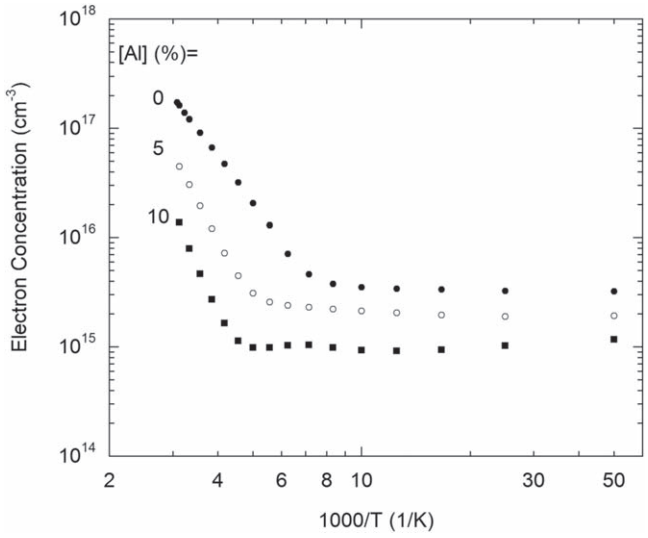

Figure 3. Temperature dependent electron concentrations in AlInAsSb for 0, 5 and 10% Al.

very similar, but as expected, the change in electron concentration as a function of the added group III element composition is slower. Due to the narrow band gaps, a substantial concentration of thermally excited electrons occurs at high temperatures. As the composition of the added group III constituent increases, the band gap increases and the free carriers decrease at a given (high) temperature, as does the nearly flat background concentration visible below ~100 K. It is important to notice, as was already mentioned, that the electron concentration in the flat region is not equal to the donor concentration, but it of course directly depends on it. In order to determine properly the actual donor concentration a full model fit, with knowledge of the temperature dependence of the band gap is required, which is beyond the scope of this work. The error is of the order of a factor of 2 [14], and can be neglected since it will not change the overall picture that emerges.

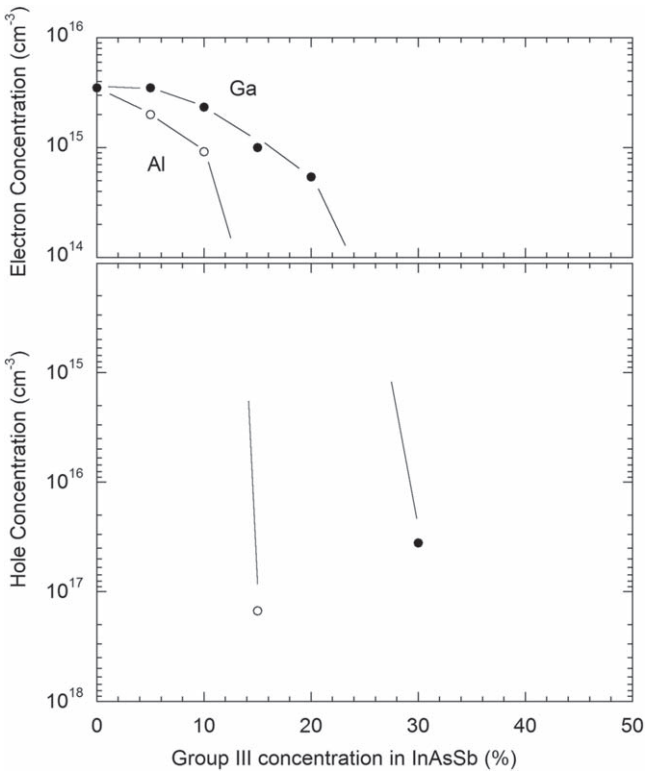

Figure 4. Free carrier concentration in AlInAsSb and GaInAsSb as a function of the added group III composition with the same lattice constants.

Figure 4 shows the low-temperature free carrier densities as a function of Ga and Al mole fractions. We observe a monotonic decrease in the free electron concentration as the added group III composition is increased with a quite abrupt type-flip beyond a critical concentration, in striking agreement with the ADM predictions.

The fact that the conduction type-flip happens in nominally undoped material strongly indicates that this behavior originates from the presence of native defects that, most likely, are associated with a small degree of film non-stoichiometry. Typically, vacancy defects accompany such non-stoichiometry. To gain further quantitative insights we set out to model their expected concentrations.

Since these alloy systems have only recently drawn attention, many of their parameters (such as the deformation potential) of the related binary semiconductors upon which these calculations are based are known only very roughly, or have only a value calculated from theory rather than a measured value. Additionally, because the relationship between the parameters of binary semiconductors and quaternary semiconductors involving the same elements is unknown, the purpose of this analysis is not to try to develop a high-precision model against which numerical experimental measurements can be compared. Instead, the purpose is to show that the n-type to p-type transition in the quaternaries can be modeled using numerical parameters that are within the bounds of those values for the related binary compounds.

We included effects of nonparabolic conduction bands and determined the positions of the conduction and the

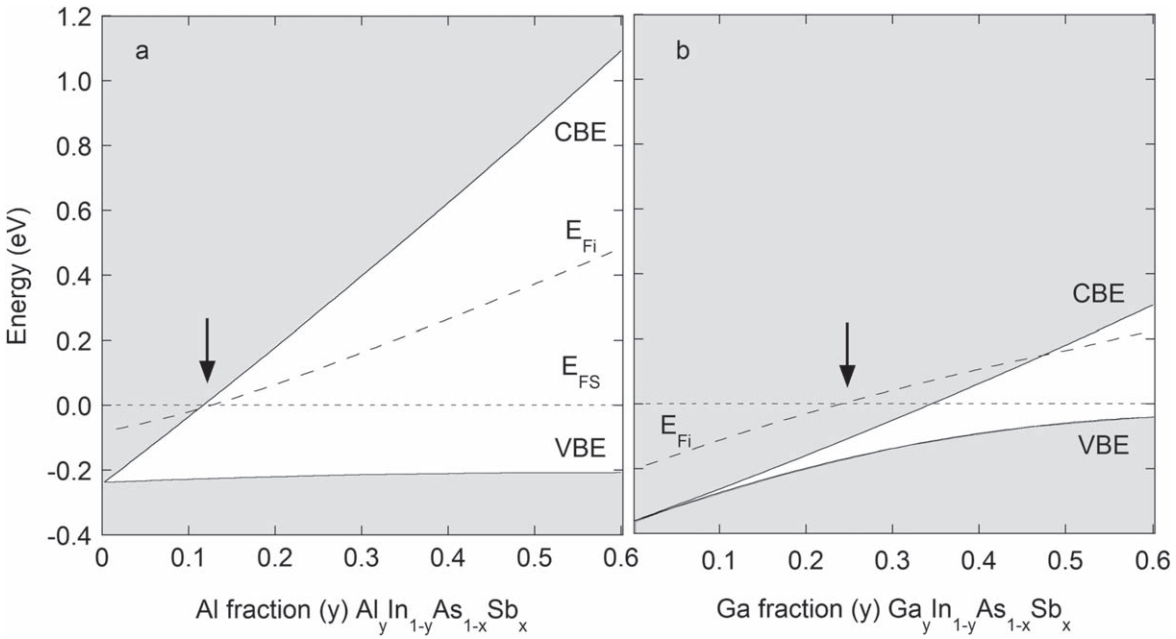

Figure 5. Conduction and valence band edges along with Fermi energy at the growth temperature (688 K) as a function of the Al (a) and Ga (b) composition for the quaternary alloys AlInAsSb and GaInAsSb. The As/Sb concentrations are adjusted to maintain lattice matching to $InAs_{0.53}Sb_{0.47}$. The arrows indicate the concentrations where $E_{FS} = E_{Fi}$.

valence band edges relative to E_{FS} as a function of temperature by interpolation from the binary materials. The temperature dependence of the conduction band edges relative to the vacuum level comes mainly from the thermal expansion of the lattice parameter [17]. We have calculated those shifts for the related binary semiconductors using equation (6) in [17], which depends on the fractional expansion of the lattice parameter and the conduction band deformation potential.

We begin with the assumptions that the material exhibits a small nonstoichiometry accommodated by the presence of amphoteric vacancy-like defects with concentration, N_d, such that

$$N_d = N_D + N_A \tag{1}$$

where N_D and N_A are donor and acceptor concentrations, related by [18]

$$\frac{N_D}{N_A} = \exp\left[-\frac{2(E_F - E_{FS})}{k_B T}\right] \tag{2}$$

In the most extensively studied case of GaAs, theoretical calculations have shown that native defects can experience large lattice relaxations and both anion and cation site vacancies undergo a Fermi energy induced transformation between donor and acceptor configuration [19, 20].

We will first assume that the transformation of the defects between their donor and acceptor configurations [7] can occur only at the growth temperature $T_{growth} = 688$ K and calculate the position of the intrinsic Fermi energies E_{Fi} , shown in figure 5. As one can see, E_{Fi} shifts from below to above E_{FS} with increasing Al or Ga content. This indicates that the defects will be driven from their donor to their acceptor configuration. The calculated crossover points are very close to the experimental results in figure 4.

Figure 6 shows the calculated donor and acceptor concentrations for different defect concentrations. Because the hole concentration in figure 4 is so much larger than the electron concentrations, N_d must be different in the different samples measured. However, even so, one can see that the qualitative behavior seen in figure 4 is well reproduced in figure 6.

The material changes from electron to hole conduction at the same alloy composition, regardless of the defect concentration, and although the carrier concentration appears to saturate or be near saturation for GaInAsSb at low Ga fractions, AlInAsSb is clearly not saturated at low Al fractions.

One of the key assumptions in our calculations was that the lowest temperature at which the defects could transform from their n-type to p-type configuration was at the growth temperature. It is quite possible that such a transformation is allowed at lower temperatures and it is worth exploring how such a difference might affect our results.

We recalculated the results of figure 6 at room temperature and found that even in this extreme case, the alloy fractions at which the intrinsic Fermi energy crosses E_{FS} are similar to those occurring under the assumption that the defect could only transform at the growth temperature. For the Al case, the crossover point is 13% (growth temperature) and 18% (room temperature). For Ga, the corresponding values are 24% and 23%. The experimental numbers are estimated to be Al = 13% and Ga = 27%, in very good agreement with the calculated values for the growth temperature.

The implication is that it is unlikely that a change in growth temperature alone could fundamentally affect the background doping *type*, although the III:V flux ratios might influence the *concentrations*.

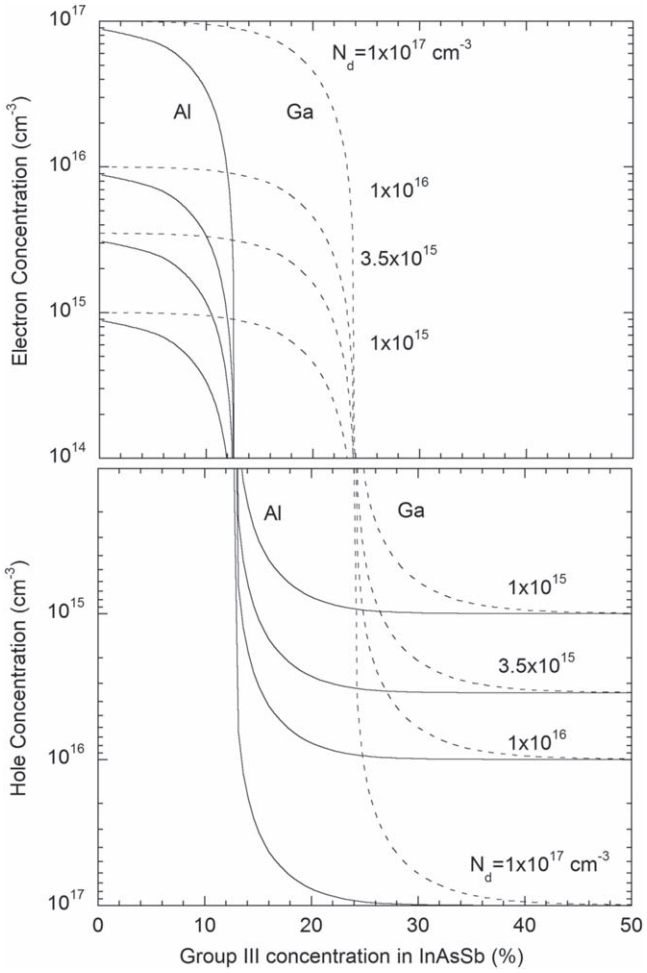

Figure 6. Calculated free carrier concentration in GaInAsSb and AlInAsSb as a function of the Ga or Al alloy composition with the same lattice constants. Curves are shown for different constant defect concentrations N_d over the relevant alloy range.

Of the specific alloys studied here, AlInAsSb is of particular interest in applications such as infrared detectors. It is a commonly used barrier layer to prevent majority carrier electrons from generating a dark-current in e.g. an InAsSb absorber. By tailoring the compositions, in principle it should be possible to eliminate any valence band barrier for holes. Nevertheless, in practice a valence band barrier appears to be present that requires an (undesirable) bias of the device. The engineering solution used is typically to add p-dopants to the barrier. In light of the observations made here, the reason for this is not that the barrier alloy is n-type. Rather, the benefits of the added extra doping are most likely to eliminate an electrostatic barrier. This can be caused by the accumulation of electrons at the interface, which is analogous to the accumulation at the surface. This is another manifestation of the importance of the E_{FS} position relative to the bands. We plan to present additional data supporting this statement in a future publication.

In summary, the experiments presented here demonstrate that the amphoteric native defect model is more than a classification tool. It describes phenomena in compound semiconductors that appear to be fundamental. If allowed by the available range of band edge positions, the ADM can be used to design materials with desired background type. The ADM is part of a closely related fundamental set of observations that describe lattice constants, bandgaps and their relative positions, surface and interface pinning energy levels, and doping characteristics.

Acknowledgments

The expert support by Mr Gregory P Meissner in the preparation of the samples is recognized. The work in Berkeley was performed in the Electronic Materials Program and was supported by the Director, Office of Science, Office of Basic Energy Sciences, Materials Sciences and Engineering Division, of the US Department of Energy under Contract No. DE-AC02-05-CH1123.

ORCID iDs

Stefan P Svensson https://orcid.org/0000-0002-2600-0987

References

[1] McCaldin J O, McGill T C and Mead C A 1976 *Phys. Rev. Lett.* **36** 56
[2] Capasso F and Margaritondo G 1987 See for example heterojunction band discontinuities *Physics and Device Applications* (Amsterdam: North Holland)
[3] Hakala M, Puska M J and Nieminen R M 2002 *J. Appl. Phys.* **91** 4988
[4] Sato Y and Sato S 1994 *J. Crystal Growth* **144** 15
[5] Walukiewicz W 1987 *J. Vac. Sci. Technol.* B **5** 1062
[6] Walukiewicz W 1989 *Appl. Phys. Lett.* **54** 2094
[7] Walukiewicz W 2001 *Physica* B **302–303** 123
[8] Tejedor C, Flores F and Louis E 1977 *J. Phys.* C **10** 2163
[9] Tersoff J 1984 *Phys. Rev. Lett.* **52** 465
[10] Vurgaftman I, Meyer J R and Ram-Mohan L R 2001 *J. Appl. Phys.* **89** 5815
[11] Alberi K and Scarpulla M A 2016 *Sci. Rep.* **6** 27954
[12] Walukiewicz W, Rey-Stolle I, Han G, Jaquez M, Broberg D, Xie W, Sherburne M, Mathews N and Asta M 2018 *J. Phys. Chem. Lett.* **9** 3878
[13] Svensson S P, Crowne F J, Hier H S, Sarney W L, Beck W A, Lin Y, Donetsky D, Suchalkin S and Belenky G 2015 *Semicond. Sci. Technol.* **30** 035018
[14] Svensson S P, Beck W A, Sarney W L, Donetsky D, Suchalkin S and Belenky G 2019 *Appl. Phys. Lett.* **114** 122102
[15] Svensson S P, Sarney W L, Donetsky D, Kipshidze G, Lin Y, Shterengas L, Xu Y and Belenky G 2017 *Appl. Optics* **56** B58
[16] Sarney W L, Svensson S P, Donetsky D and Belenky G To be published
[17] Welna M, Baranowski M, Kudrawiec R, Nabetani Y and Walukiewicz W 2017 *Semicond. Sci. Technol.* **32** 015005
[18] Walukiewicz W, Rey-Stolle I, Han G, Jaquez M, Broberg D, Xie W, Sher-burne M, Mathews N and Asta M 2018 *J. Phys. Chem. Lett.* **9** 3878
[19] Baraff G A and Schlüter M 1985 *Phys. Rev. Lett.* **55** 1327
[20] Baraff G A and Schlüter M 1985 *Phys. Rev. Lett.* **55** 2340